Seismic Vulnerability of the Italian Roadway Bridge Stock

Barbara Borzi,[a] Paola Ceresa,[b] M.EERI, Paolo Franchin[c], Fabrizio Noto[d], Gian Michele Calvi,[b] M.EERI, Paolo Emilio Pinto[c]

This study focuses on the seismic vulnerability evaluation of the Italian roadway bridge stock, within the framework of a Civil Protection sponsored project. A comprehensive database of existing bridges (17,000 bridges with different level of knowledge) was implemented. At the core of the study stands a procedure for automatically carrying out state-of-the-art analytical evaluation of fragility curves for two performance levels – damage and collapse – on an individual bridge basis. A webGIS was developed to handle data and results. The main outputs are maps of bridge seismic risk (from the fragilities and the hazard maps) at the national level and real-time scenario damage-probability maps (from the fragilities and the scenario shake maps). In the latter case the webGIS also performs network analysis to identify routes to be followed by rescue teams. Consistency of the fragility derivation over the entire bridge stock is regarded as a major advantage of the adopted approach.

INTRODUCTION

In Italy most of the bridges along the roadway network have been built in the '60s and '70s (Pinto and Franchin 2010), almost exclusively in reinforced (RC) or pre-stressed concrete. In spite of the rather primitive seismic design regulations in force at the time (low, nominal forces with no capacity design provisions) the generally conservative bridge design practice resulted in a moderate seismic vulnerability against collapse observed in the last major events (from Irpinia 1980 to Emilia 2012). Lower degrees of damage, however, causing closure to general traffic and in some cases even to emergency traffic, were instead observed.

[a] Centro Europeo di Formazione e Ricerca in Ingegneria Sismica (Eucentre), Via Ferrata 1, 27100 Pavia, Italy
[b] Istituto Universitario di Studi Superiori di Pavia (IUSS), Piazza della Vittoria 15, 27100 Pavia, Italy
[c] Università degli Studi di Roma "La Sapienza", Via Gramsci 53, 00197 Roma, Italy
[d] METIS s.r.l., Via Emanuele Filiberto, 00185 Roma, Italy

This paper presents results of a research project funded by the Italian Civil Protection Department with the general goal of assessing the seismic risk of the Italian road transportation network, to highlight retrofit priorities, and to allow real-time scenario evaluation for the purpose of emergency rescue operations. At the current state of the development, documented in this paper, only the vulnerability of bridges is taken into account, while that of tunnels, retaining walls and other network elements will be considered in future developments. Further, within the bridges stock, only RC girder bridges are considered, since (simply supported or continuous) bridges of this type are by far the prevalent typology (>90%) in the stock (Pinto and Franchin 2010).

Other seismic risk assessment studies have been undertaken on the Italian highway network in the past. Pinto et al. (1996) carried out a project focusing on the bridges of the highways managed by "Società Autostrade". More recently the S.A.G.G.I. project (Nebbia and Pardi 2008) analyzed bridges of the same network, now managed by the private concessionaire "Autostrade per l'Italia" s.p.a., and the applied methodology was tested on ten selected structures. The VIA project (GNDT 2000) assessed the seismic risk along a small portion of the network, the motorway between Avellino and Benevento in Southern Italy, that was struck during the 1980 Irpinia event and subsequently retrofitted.

The novelty of the present study is mainly related to its scope, which extends to the entire Italian roadway bridge stock, regardless of the fact that they are maintained/managed by an institutional owner or a private concessionaire, and to the method for fragility derivation which abandons the typological fragility approach in favor of a bridge-specific one. As a consequence of the scope of the research, the vulnerability assessment of the bridges has been undertaken accepting a priori the fact that the level of knowledge of the bridges could not be homogeneous. The main differences are due to the large number of managing authorities in play having stored information on their own structures in various databases that range from electronic to conventional paper archives or hybrid ones (Figure 1, which depicts all steps and elements in the vulnerability study). The first task has been therefore that of devising a unified comprehensive database (DB) to store nonhomogeneous information on the bridges.

This paper provides a description of the available data, presents the methodology for assessing the vulnerability of the bridges and for the evaluation of seismic risk and real-time damage scenarios, the development of the automatic procedure for fragility analysis and the

web platform with GIS (Geographical Interface System) functionality used to visualize and manage data and results.

AVAILABLE DATA AND DEVELOPED DATABASE

The adopted methodology for the fragility assessment of the bridges is based on inelastic response history analysis (IRHA). In order to define finite element (FE) models of the bridges suitable for performing IRHAs, a relational DB with a comprehensive structure has been implemented.

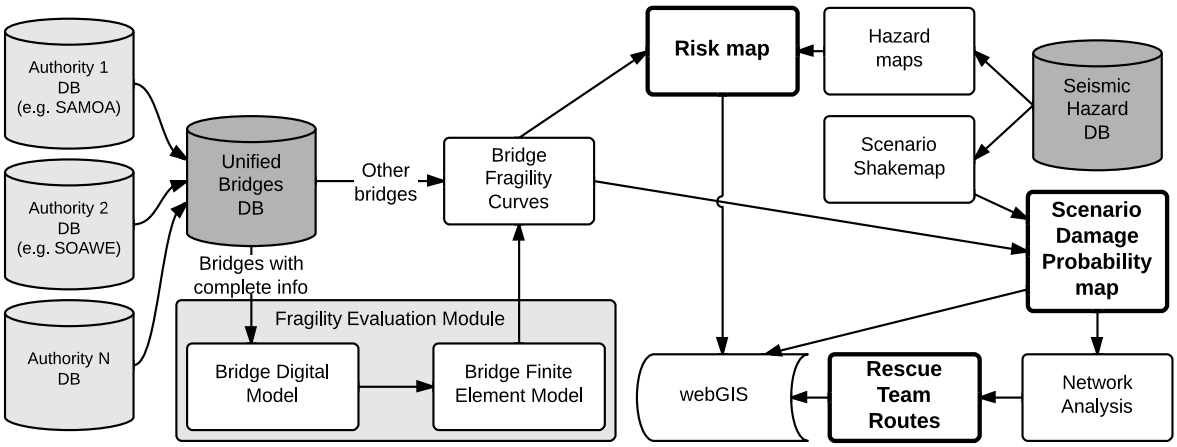

Figure 1. Overall description of the seismic vulnerability assessment study of the roadway bridge stock in Italy.

The DB is first queried by the fragility evaluation module in order to build a digital model of the bridge, termed Bridge Information Model (BIM). The latter defines geometry, loads, seismic masses and nonlinear properties of elements and supports, from which FE models of the bridge are generated to perform IRHA (Figure 1). The structure of the relational DB set up to store the bridges' information (Unified Bridges DB in Figure 1) is shown in the electronic supplement materials (Figure A-1).

During the course of the project it was not possible to retrieve the above indicated amount of data for all the bridges in the network. ANAS, the national authority that owned all state roads and bridges within, in recent years has devolved many state roads, re-classified as either regional or provincial, to regions and provinces. Moreover, highways have been privatized and split in no less than 26 concessionaires. This process resulted in a very fragmented base of information. As such the ANAS cadastre contains basic data for the whole territory but it is not exhaustive and must be complemented by provincial data sets and the highway concessionaires data sets. The unified DB has been populated so far with about

17,000 bridges (mostly location data), from three sources: the Catasto (cadastre) and SOAWE DBs from ANAS, and the DB from Province of Trento in the North-East (see the white circles in Figure 2). In conclusion, a complete set of data – in terms of geographical location, geometry and structural data – is available only for the 485 bridges of ANAS Soawe DB (see the black circles in Figure 2).

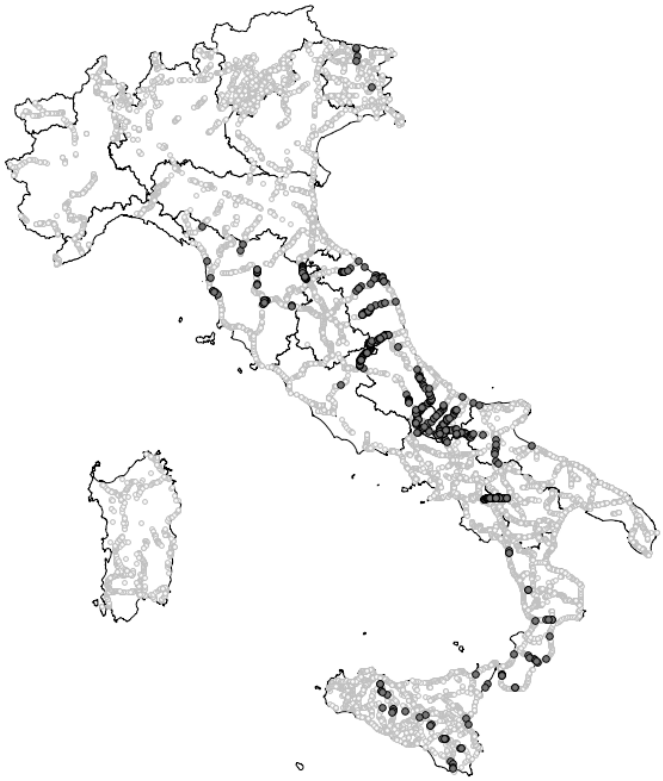

Figure 2. Bridges in the available DBs: the black circles represent the 485 bridges with a complete set of data, the white circles are related to the other bridges with mainly location data.

Figure 3 shows a sample of the distribution of properties on the 485 bridges of the SOAWE DB. From top left to bottom right, the figure shows the number of spans, the minimum and maximum height of piers, the prevailing soil category under the supports (according to Eurocode 8 classification), the foundation type, the type of deck and piers, the piers cross section and the bearing typology. By far the most frequent characteristics are less than 5 spans, single-stem piers between 10 m and 20 m high with box-type section, piled foundation on B soil category, and simply supported decks on thin elastomeric pads.

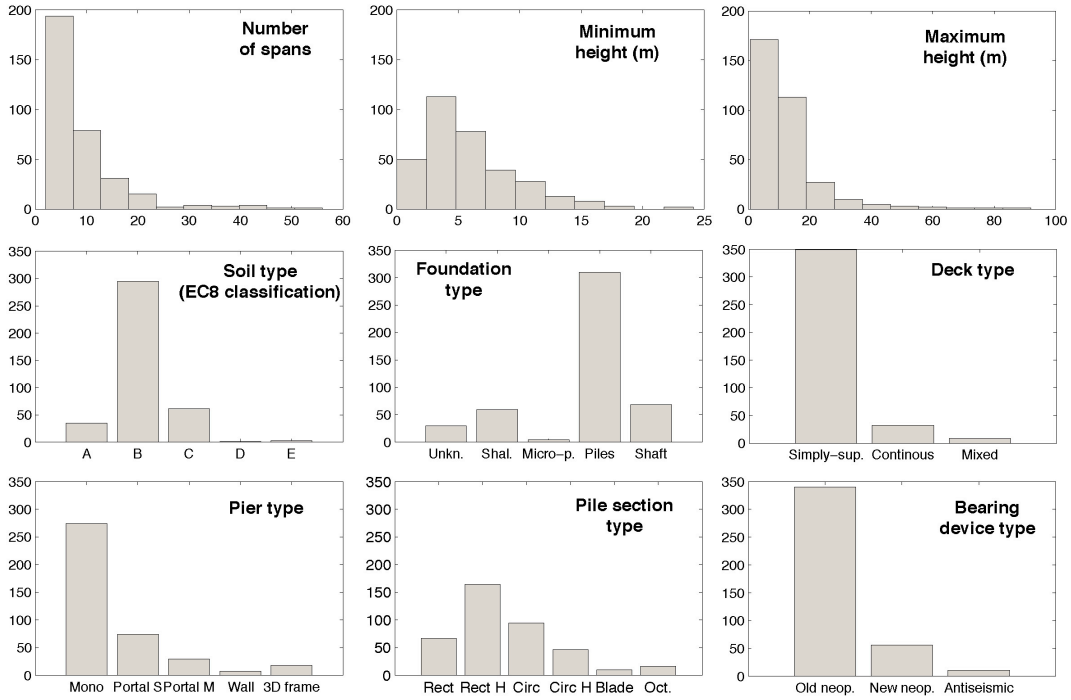

Figure 3. Distribution of properties on the 485 bridges of the ANAS Soawe DB.

ADOPTED METHOD FOR BRIDGE VULNERABILITY EVALUATION

The long-term goal of the study, i.e. a consistent evaluation of bridge-specific fragility curves on a bridge stock of several tens of thousands of bridges over the entire national territory, requires a procedure that can be automatically applied. This requirement has forced some choices, especially on the seismic input side but also on the treatment of uncertainty, that would not be optimal according to current state of the art of research. These choices are discussed in the following sections.

As previously stated, the adopted method for fragility assessment is based on IRHA. The fragility curve is obtained point-wise for nine increasing values of peak ground acceleration (PGA). The latter is selected as the optimal measure of ground motion intensity. Bridges are plan-extended structures characterized by a number of significant vibration modes, each one contributing to the dynamic response of a different portion of the structure. Therefore any scalar IM lacks the necessary sufficiency. If one bridge only were to be analyzed, one could consider a vector IM including the spectral acceleration at all significant periods, but when risk assessment of a bridge portfolio is undertaken, PGA, in spite of it being not optimal for any bridge, is the simpler common denominator. Besides, recent research has shown that

sensitivity to the IM choice is negligible when an appropriate (complementary to the IM) suite of motions is employed for the IRHA (Bradley 2013)(Lin et al. 2013).

The nine PGA values are characterized by increasing mean return period of exceedance T_R, from 30 to 2475 years. These are the values for which the current Italian building code (DM 14/10/2008) specifies elastic acceleration response spectra on a 0.05°×0.05° (~5 km) grid covering the entire national territory.

At each intensity level *m* (multi-component) artificial motions are produced to match in the mean the associated code-given elastic spectrum. IRHA under these motions provides a small sample of response corresponding to demand values *D* in each bridge component. These are compared with the corresponding component capacity values *C* (depending on the considered performance level, see later) sampled from their respective distributions. The obtained sample of the component demand to capacity ratios *y=D/C* can be used to obtain a global, structural system level *D/C* ratio denoted by *Y* (Jalayer et al. 2007). For simple structural systems, such as those of girder bridges, a simple "series system" scheme is adequate (the weakest failure mode determines global failure) and hence the global *D/C* ratio for the *j*-th intensity level and *k*-th motion is given in terms of the *n* local *D/C* ratios by:

$$Y_{jk} = \max\left(y_{1jk}, \ldots, y_{njk}\right) \quad j = 1, \ldots, 9; \quad k = 1, \ldots, m \tag{1}$$

The *m* values of *Y* at each intensity level are used to fit a conditional lognormal distribution, by estimating log-mean $\mu_{\ln Yj}$ and log-standard deviation $\sigma_{\ln Yj}$, and to determine the probability of exceedance of the unit value of *Y* that marks the attainment of the performance level *D=C*. This is the fragility value at the *j*-th intensity level:

$$p\left(Y > 1 \middle| j\right) = 1 - \Phi\left(\frac{\ln 1 - \mu_{\ln Yj}}{\sigma_{\ln Yj}}\right) \tag{2}$$

The procedure is often called a multiple-stripe analysis (MSA) (Jalayer and Cornell 2009), and is similar in concept to incremental dynamic analysis (IDA) (Vamvatsikos and Cornell 2002) with the important difference that it does not require or requires only limited scaling (when natural motions are used) and that it can use different suites of motions at each intensity level thus reflecting the change in source parameters (hazard de-aggregation) occurring when moving to different intensities. Finally each fragility curve is fitted through least squares with a lognormal CDF shape (as shown in Figure 4).

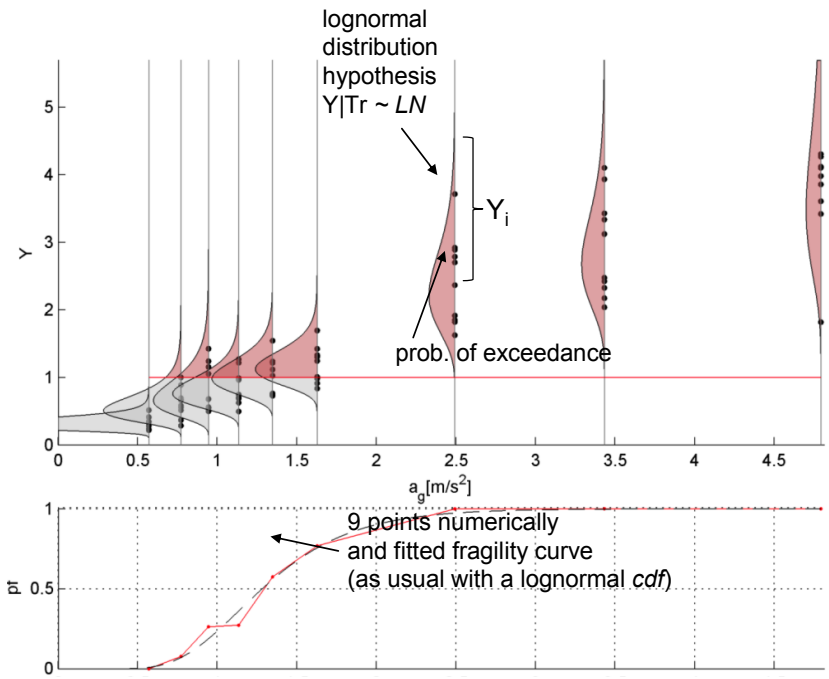

Figure 4. Procedure for fragility assessment. Top: sample values of the global *D/C* ratio *Y* and fitted lognormal distribution conditional on intensity level (here the peak ground acceleration a_g is used). Bottom: fragility curves and lognormal fit.

An important aspect of the chosen procedure is that the stripes are in a fixed number of 9 for pre-defined return periods (max 2475 years) and, thus, in most areas the associated intensities are such that the response is still far away from the collapse thresholds (see later). As a result, the collapse fragility is often traced only in its first portion (left tail).

The ad-hoc application developed for computing the fragility curves of the bridges, called BRI.T.N.E.Y (BRIdge auTomatic Nonlinear analysis based Earthquake fragilitY) performs queries to read the DB data and creates its BIM and FE models for carrying out analysis with OpenSees (McKenna et al. 2010). The post-processing of the results is also carried out by the same automatic application, as it will be explained in the following Sections and in the electronic supplement materials.

MODELING

In general a bridge is made up of a single carriageway, although in special cases such as that shown in Figure 5, the bridge can have multiple carriageways supported on the same sub-structure. The application allows for these cases and requires that additional carriageways be defined relative to the first one (start point and orientation). Each carriageway is defined as a sequence of span segments, grouped in spans and decks. The reasons for subdividing spans in segments are for better discretization of masses and to allow

for section changes, internal releases, change in plan orientation (typically curves). In the latter two cases the segments are generated automatically. At the separation between decks two coincident but not connected nodes are generated to allow for relative displacements (for abutments, the latter are computed relative to a fixed node at the start of the first deck and the end of the last deck). Double coincident nodes are used also for internal releases, like Gerber saddles. There is no need to specify the substructures positions that are inferred by the end/start points of the decks.

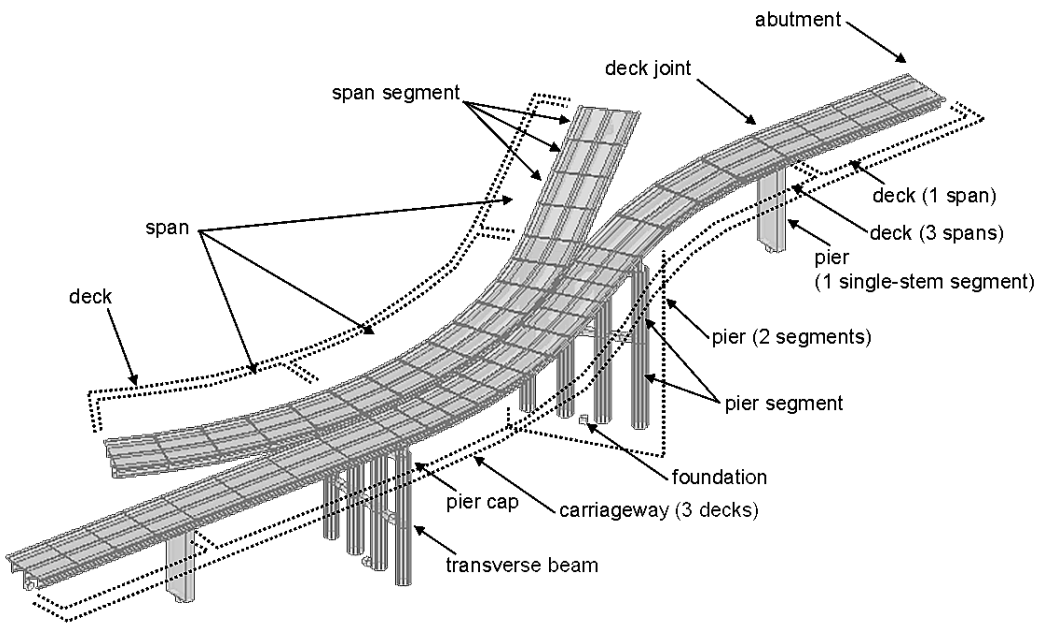

Figure 5. Elements in the Bridge Information Model (BIM) for one of the DB bridges.

The created elements (see Figure 6) are either frame elements, *Elastic* for the deck and *BeamWithHinges* (the flexibility-based element with internal elastic portion and two nonlinear end hinges with Gauss-Radau integration by Scott and Fenves 2006) for the pier segments and the transverse beams, respectively, or *zeroLength* elements for deck connections and *twoNodeLink* elements for bearing devices within super- to sub-structure connections. Inelasticity is modeled within both frames and *zeroLength* elements. For this purpose, in the *beamWithHinges* elements the cross-section is discretized into fibres. A large library of section shapes and associated reinforcement layouts allows for only a minimum amount of information to be stored in the DB. *RigidLink* elements are also used to model connections (see Figure 7). Uniaxial constitutive models employed for the fibre section of inelastic elements are the Scott-Kent-Park concrete model (*Concrete01* in OpenSees) and the bilinear steel model (*Steel01* in OpenSees). Values for the material models parameters are established for each of the 485 analyzed bridges based on available material testing reports.

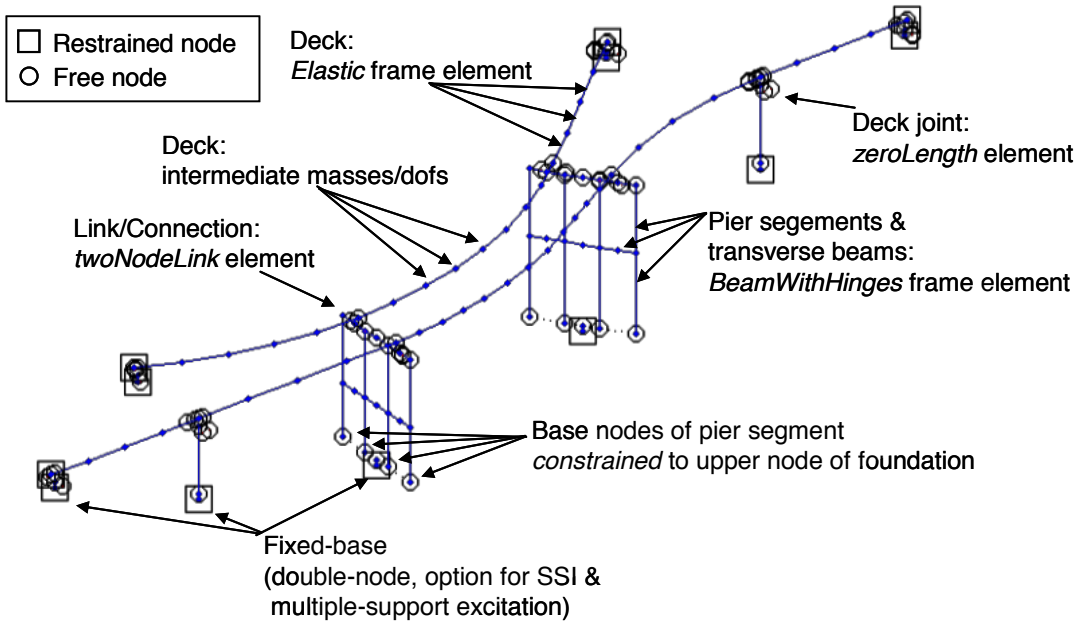

Figure 6. Elements in the Bridge Finite Element Model for one of the DB bridges.

Connections between super- and sub-structure are specified at the start and end of each span. Two adjacent spans can be connected to the same sub-structure. The geometric quantities used to describe the connection are (see Figure 7): the horizontal and vertical distances ΔL and $\Delta Z = \Delta Z_G + \Delta Z_C$, the skew angle, the number and spacing of bearing devices. If the number of bearings is zero the connection is assumed to be rigid (the piers frame into the deck), otherwise a force-deformation relationship must be specified for the horizontal degrees of freedom of the devices (the vertical degree of freedom and the rotations are assumed to be rigid and infinitely flexible, respectively). Available force-deformation laws in OpenSees (e.g. Elastomeric, FlatSlider, FrictionPendulum) cover the full spectrum of devices, traditional and modern, to be found in the Italian bridge stock.

A special mention is due to the most widely used typology of bearings adopted in bridges built until the '70s (Pinto and Franchin 2010), i.e. the thin un-reinforced neoprene pads. These bearings are usually subject to high compressive stresses and, according to recent tests (Capozzi 2009), exhibit a frictional behavior right after an almost negligible elastic response, with very low friction coefficients (~10%) and up to their limited strength. There is however large uncertainty on their post-peak behavior. For this reason, the application performs two analyses, when friction element of this type are present (at the super-/sub-structure connection as well as within deck releases, including Gerber saddles), one with the low friction coefficient, to maximize relative excursions and evaluate the unseating limit state, and a second with a rigid connection, to maximize forces transmitted to the sub-structure.

A pier can be composed of any sequence of segments, BRI.T.N.E.Y. automatically generates the joints and the constraints needed to glue together segments. Figure 7, left, shows an example of a pier, which starts with a single stem and has a lighter upper portion (the figure shows that the pier-deck connection is different for the two framing spans, with three bearings on one alignment and two in the other). Pier caps are modeled as a load and mass for single-stem piers, or explicitly, as in frame piers.

Abutment and pier foundations can be modeled within the application as follows. A rigid link connects two nodes, one at the pier or abutment wall base, and the other at the foundation mat base. The inertia associated with the mat is attributed to the second node. The latter node is linked through a ZeroLength element to a coincident node, which is fixed to the external support. The ZeroLength element is used in a sub-structuring approach to model the dynamic impedance of the soil-foundation system (Figure 7, right). For the purpose of time-domain IRHA, the frequency-dependence of the impedance is approximated through assemblies of springs, dashpots and fictitious masses. The assemblies depend on the foundation typology. Solutions by Taherzadeh et al. (2009), Wolf (1991) and Gazetas et al. (1993) are adopted for piled, shallow-foundations and caissons (modeled as embedded foundations), respectively. The corresponding stiffness, damping and mass terms are attributed to the degrees of freedom of the ZeroLength element. Ground motion is input to the structure as a motion-proportional force/moment in each degree of freedom of the mat-base node (to model radiation damping).

Using different forces at each support one could account for differential inputs due to wave propagation, loss of coherence and, most importantly, different site amplification and filtering by the foundation at each support, see for example (Pinto and Franchin 2010)(Sextos et al. 2003a,b).

For the 485 analyzed bridges, however, lack of the necessary data on the foundation system did not allow exploiting the modeling capabilities implemented in the fragility module. Information was limited for most of the 485 bridges to foundation typology and maintenance reports showing no evidence of any foundation-related problem over the years. Besides, this was not considered a major issue for the purpose of the risk assessment of the bridge portfolio, for a number of reasons. The first reason is that bridge foundations are traditionally designed with a significant conservatism in Italy (Calvi et al. 2013).

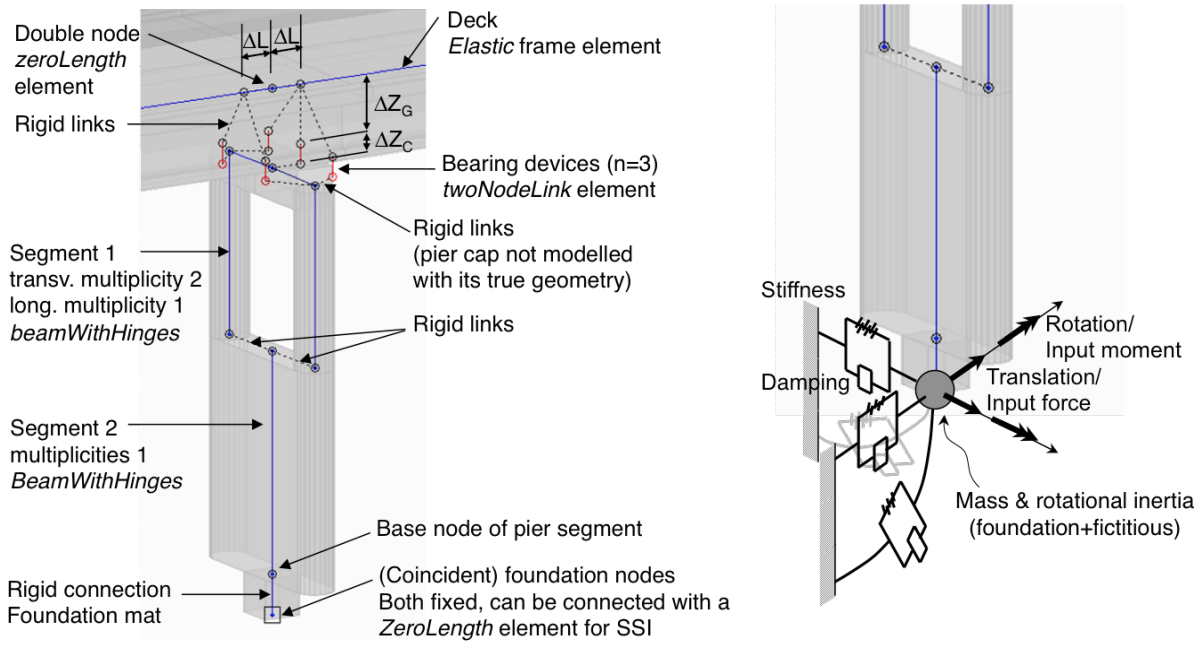

Figure 7. Finite element model: connections and sub-structures (left) foundation impedance model and input (right).

Further, systematic failure of inadequate deck-pier connections, as observed in all recent events (Pinto and Mancini 2009)(Calvi et al. 2010)(Franchin et al. 2013), limits the forces transmitted to the foundations. Finally, the third reason is that SSI has been shown to be less important than differential input (Franchin and Pinto 2010)(Sextos et al. 2003a,b). Hence, the authors feel that, in order to improve the model of the bridge, priority should be given to the differential input, also not considered at this stage of development. All the results in this study are therefore based on fixed foundation assumption, where the ZeroLength element is replaced by a kinematic body constraint. The reason for carrying out fragility analyses with a uniform excitation, corresponding to the worst soil category at the supports, is simply in recognition of the difficulty of predicting the values of the parameters of current models for simulation of differential input.

SEISMIC INPUT

The number of levels chosen for the MSA, as already mentioned, is dictated by the availability from the Italian design code (DM 14/10/2008) of the seismic hazard in terms of acceleration response spectra for 9 T_R on a fine grid over the entire national territory. The adopted spectral shape in the code is the Eurocode 8 one, with the three parameters PGA, maximum amplification F_0 (= $S_{a,plateau}$/PGA) and corner period on rock/stiff soil T_C^*, obtained as best-fit to uniform hazard spectra and tabulated for every node of the grid and T_R. By

means of BRI.T.N.E.Y., 9-suites of *m*-simulations are carried out for each bridge. Artificial, spectrum-matching motions (±10% tolerance on their mean, in the period range from 0.1s to 4.0s) are obtained with the common iterative procedure that derives a power-spectrum compatible with a target response spectrum (Muscolino 2002). The results of this large scale vulnerability assessment have been derived using 10 simulations (i.e., 10 couples of artificial horizontal records, generated for being statistically independent in x and y directions) for each intensity level (90 simulations for each bridge). Validation on both the number of motions and the difference with natural recorded motions have been carried out and presented in the following Sections.

PERFORMANCE LEVELS AND ASSOCIATED CAPACITY THRESHOLDS

Discretization of the response range in a number of damage states requires the definition of increasing response thresholds. The number of damage states chosen in different studies varies from five (NIBS 1999)(Mander and Basoz 1999), to three (Mackie and Stojadinovic 2007)(Franchin and Pinto 2009). The difficulty with the definition is the association between physical damage and numerical response thresholds (Mander and Basoz 1999)(Mackie and Stojadinovic 2007)(Franchin and Pinto 2009).

In this study two performance levels or limit states (LS) are considered both adequate for the purpose of connectivity analysis over the damaged road network and consistent with current resolution of damage predictions via numerical analysis: these are *damage* and *collapse*. The methodology previously described for computing fragility curves is therefore applied twice, with different response threshold (capacity) values.

Before discussing the actual thresholds adopted for each LS, a note is due on the general approach adopted for performance evaluation. Recently, advanced models for describing inelastic behavior of RC elements up to the very exhaustion of their deformation capacity, accounting for complex interaction between internal stresses (axial force, bending moment and shear) have been proposed (Elwood 2004)(Haselton et al. 2008), and even used in pilot fragility studies for buildings (Baradaran Shoraka et al. 2013)(Haselton et al. 2011). These models, however, are not supported by an experimental basis adequate to confer them sufficient generality, and do not possess yet the level of computational robustness needed for an unsupervised automatic fragility evaluation such as that described in this work. For this reason the choice has been made not to simulate collapse modes but to check them instead

through post-processing. Local *D/C* ratios employed for this purpose are defined for piers and bearings only. The deck, considered relatively less vulnerable, is not included in the set. Pier foundations and abutments are also not included in the vulnerable set, even though this cannot be justified in all cases based on relatively lower vulnerability, but is generally true due to a traditional conservative design of these components in the Italian bridge engineering practice (as previously discussed).

Piers can fail because either shear strength V or deformation capacity, in terms of chord-rotation θ, is exceeded. Unseating failure, which involves the deck and the sub-structure, is checked at the bearing level: bearings can fail due to excessive displacement demand d. Bearings' failure can lead to the simple fall of the deck from the bearing seat or to the full loss of support from the pier head. The first condition detects a damage LS, while the second a collapse LS.

Displacement capacity of bearings is derived from the pier cap and bearing seats geometry and considered as deterministically known. Capacity thresholds for RC piers components are modeled as lognormal random variables, as shown in Table 1. For flexure, medians are obtained from (unbiased) models specified for assessment in Eurocode 8 Part 3 (EC8-3) and reported in detail in (Biskinis and Fardis 2010a, b). The latter references provide also measures of the associated model error (sigma of the logarithm in the table).

Two response thresholds are considered for chord rotation (yield θ_y and ultimate θ_u). The shear span $L_V = M/V$ is taken equal to L for single-stem cantilever piers, or in the longitudinal direction, and $L/2$ in the transverse direction of multiple stem piers. Yield and ultimate curvatures are determined automatically from a bilinear fit of a section moment-curvature analysis to deal with general cross-section shapes and reinforcement layouts.

Shear failure is a brittle type of failure that occurs without the bridge exhibiting any sign of damage before its failure. Member failure takes place suddenly when the shear capacity of the RC section is exceeded by the seismic demand. Therefore, only the collapse LS was defined for the shear capacity of the piers. For shear the format shown in Table 1 is used, with contributions to shear strength from concrete, axial force and transverse steel that can be computed according to three different models (Kowalsky and Priestley 2000)(Biskinis et al. 2004)(DM 14/01/2008)(Biskinis and Fardis 2010a, b). The model error value in the table is appropriate for both (Kowalsky and Priestley 2000) and (Biskinis et al. 2004), and has also been used for the model in (DM 14/01/2008).

To account for the bi-directional response under multi-component seismic input, the local *D/C* ratios y_i are defined in terms of the one-directional ratios as the SRSS combination (elliptical interaction surface) or the maximum (rectangular interaction surface), for the piers and bearings, respectively. For example, the local ratio for flexural deformation at the collapse LS is given in terms of the responses and capacities in the longitudinal (*L*) and transverse (*T*) directions (these are meant with respect to the component local reference) by Eq.(3).

Table 1 Capacity thresholds for pier segments (h and d_b are the section height and longitudinal bar diameter, respectively).

LS	Mechanism	Median	$\sigma_{\ln}$
Damage	Flexure	$\theta_y = \phi_y \frac{L_V}{3}$	0.30
Collapse	Flexure	$\theta_u = \theta_y + (\phi_u - \phi_y) L_p \left(1 - \frac{L_p}{2L_V}\right)$ with $L_p = 0.1L_V + 0.17h + 0.24\frac{d_b f_y}{\sqrt{f_c}}$	0.40
	Shear	$V_u = V_c + V_N + V_s$	0.25

$$y_{i,\theta u} = \sqrt{\left(\frac{\theta_{iL}}{\theta_{uiL}}\right)^2 + \left(\frac{\theta_{iT}}{\theta_{uiT}}\right)^2} \tag{3}$$

Limited experimental evidence supporting the use of the SRSS directional combination for detecting failure in bi-axial bending/shear is reported in (Biskinis and Fardis 2010a, b).

As already mentioned, the global *D/C* ratio *Y* is then obtained as the maximum over all local ratios, i.e. over components (piers and bearings) and mechanisms (flexure, shear, unseating).

TREATMENT OF UNCERTAINTY

Uncertainty in seismic input, material properties and capacity models is considered in the procedure. The former is modeled by means of ten artificial signals at each intensity level. The latter, as explained in the previous section, is modeled with lognormal random variables with unit median (unbiased models) and log-standard deviation equal to that provided for the employed capacity model, which usually accounts for model error (hidden variables, model form). Statistical uncertainty in the model parameters, see e.g. (Gardoni et al. 2002)(Zhu et al. 2007), has not been included since in most cases is not available.

Material properties, and in particular concrete strength f_c and steel yield stress f_y, are modeled with lognormal random variables.

Due to the large-scale of the vulnerability assessment, simplifying choices have been made in all three cases. Those regarding the input motions have already been discussed. Two additional approximations have been introduced with reference to capacity models and material properties.

First of all, since collapse modes are not simulated but checked a posteriori, response thresholds are not introduced in the model (elements will deform beyond θ_u and will not start degrading at V_u). Hence, random model error terms of response thresholds appear only at the denominator of ratios such as that in Eq.(3). Further, these error terms in principle have both an inter-element and an intra-element component, meaning that some of the associated variability is due to hidden variables which take the same value across similar elements, and the rest is associated with variables that differentiate apparently similar elements. As a result there should be a vector of error terms of length equal to the number of elements, characterized by a correlation matrix. Since only the total variance is given for available capacity models, the assumption of perfect correlation is made within the same mechanism.

Material properties should also be different for each element, and modeled for instance as spatial random fields with a mean, variance and auto-correlation function. Each property is instead described with a single random variable assuming perfect correlation and uniform variance. Contrarily to model errors, however, these variables appear in both the numerator and denominator of the *D/C* ratio, since they are used in the capacity formulas and in the FE model. Again, in a way of simplification and to limit the computational burden, rather than considering the complete set of combinations of input uncertainty and structure-related uncertainties (like e.g. in Dolsek 2009), a single sample of material properties is associated with each artificial motion. The procedure results in an inflated response variance and a possibly reduced median intensity causing the limit state (Liel et al. 2009).

VALIDATION OF AUTOMATIC PROCEDURE AND OTHER ASSUMPTIONS

The validation process carried out during this work was mainly focused on the verification of the automatic generation of the FE bridge model from the DB data, the automatic manipulation of the results during the post-processing and the computation of the fragility, as well as on the evaluation of the influence of the number m of simulations per

each intensity level, and the use of natural motions rather than artificial ones in order to appreciate the possible impact on the evaluated fragilities.

The first steps of the validation were related to the verification of the automatic procedures carried out by BRI.T.N.E.Y. for bridge modeling and performing IRHAs using OpenSees. The results of the IRHAs automatically performed by BRI.T.N.E.Y have been contrasted with those obtained by an independent user setting up models and performing analyses within the commercial software MIDAS Civil (2011). Figure 8 shows the models of four bridges considered in the comparison. They are deemed to be representative, since they include both straight and curved bridges, a varying number of spans, single stem, wall and multiple stem piers, and different bearing devices. A sample of the results of the comparison is shown in Figure 9. The small differences are representative of the differences exhibited in all other results and are due to the different element formulations of the fibre beam-column elements in the two codes, all other things being equal.

A further point to be evaluated was related to the use of artificial motions in such a small number (10 couples of records for each intensity level) for the purpose of fragility evaluation. Sensitivity to this choice was tested considering a selected set of twelve bridges, for which the fragility curves were computed with 30 two-component artificial motions per level and compared with those obtained with 10 two-component motions only. Figure 10 shows the obtained fragility curves for the friction modeling of the devices for three of the selected bridges. No significant differences are detected (Figure 10).

Additional effects taken into account during this study were related to the use of artificial motions rather than, for examples, natural recorded ones. A set of bridges was selected and their fragility curves were also computed with natural recorded motions. REXEL (Iervolino et al. 2010), a computer code developed for record selection, was used for the purpose of finding suites of natural motions matching on average the target spectrum at each intensity level. Additional constraints, however, were used in the selection: i) elimination of very large variability of spectral ordinates; ii) the least possible amount of scaling to match the target spectrum (Bommer and Acevedo 2004); iii) records selected for a given range of magnitude and distance according to the disaggregation of hazard (http://esse1.mi.ingv.it).

Damage and collapse fragilities for three bridges were computed with 10 natural two-component and 10 artificial two-component motions. The results confirm some expected facts.

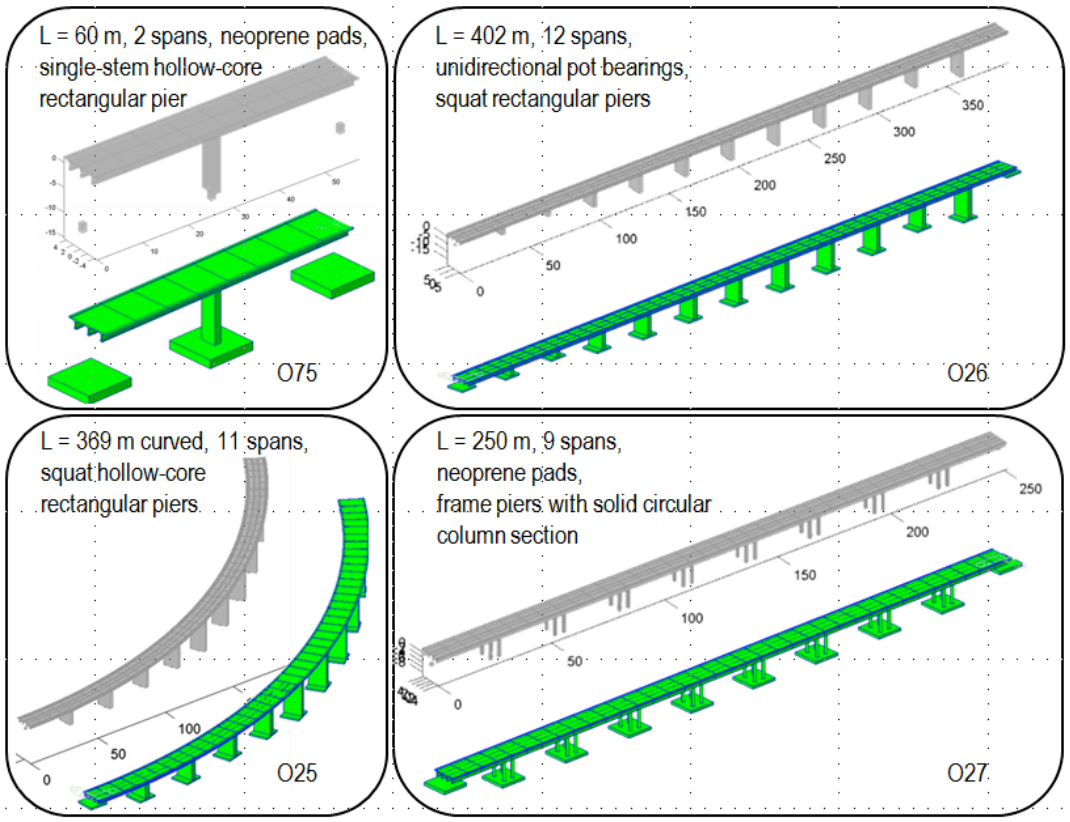

Figure 8. The bridge models (named O75, O25, O26, O27) set up by the automatic procedure BRI.T.N.E.Y (top left bridges of each window) and those set up by a user in MIDAS (bottom right bridges of each window).

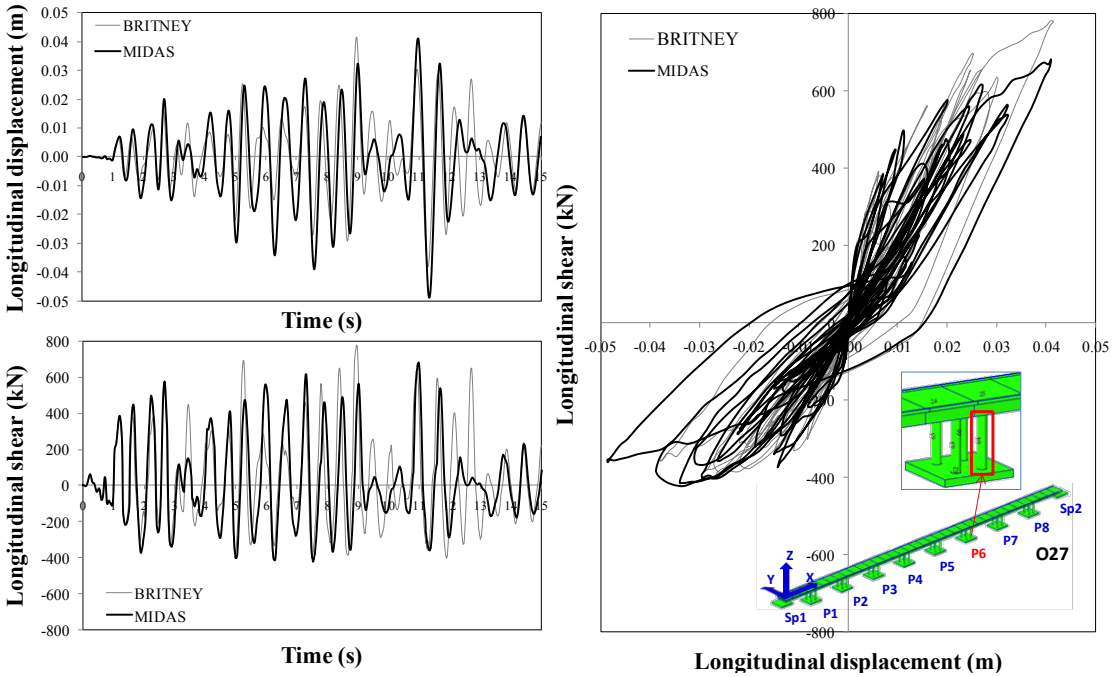

Figure 9. Sample results of the comparison between the BRI.T.N.E.Y and MIDAS models. Bridge O27 (see Figure 8), pier 6: longitudinal top displacement (top left), shear force time series (bottom left) and force-displacement loops of one of the four columns (motion in the x and y directions, PGA = 1.81 m/s^2).

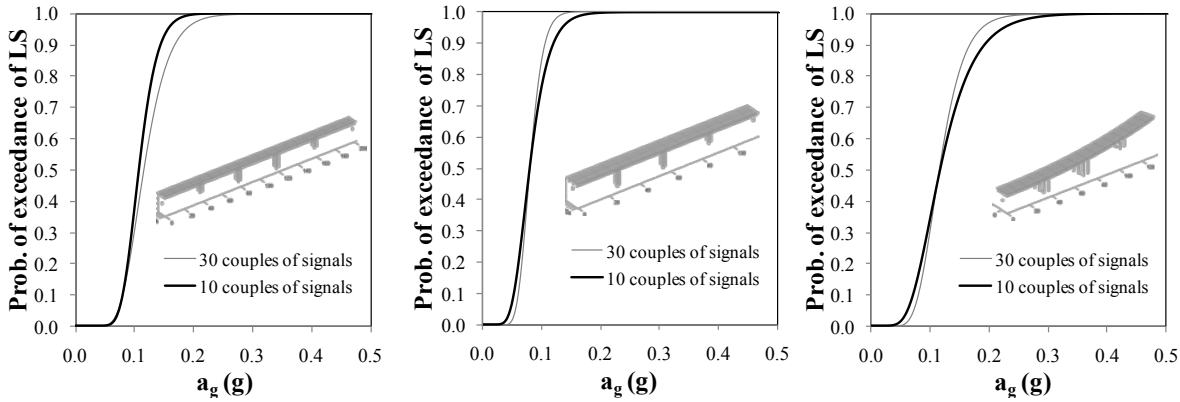

Figure 10. Fragility curves evaluated with 30 and 10 artificial motions for three of the selected bridges (named O50, O70, O220 from the left to the right hand side).

The mean response predicted with natural and artificial motions, at each intensity level, is similar (ratio of natural to artificial mean *Y* in the 1±0.25 interval), while the larger input variability proper of natural motions induces a larger response dispersion. These differences are generally smaller and do not impact much on the damage fragility. The collapse fragilities are instead more conservative if artificial accelerograms are used (when medians are indeed lower). This is an expected outcome, since the frequency content of artificial accelerograms is more severe than that of natural accelerograms. The differences, which are non negligible as expected, are accepted for the purposes of the large scale vulnerability assessment and the need for a consistent evaluation.

The validation studies on both the number of motions and the difference with natural recorded motions have confirmed than 10 artificial motions are acceptable for the damage LS fragility curve. Their adequacy for the collapse LS is lower, as expected, even though the comparison is comparatively more difficult since it is usually done on the left tail (i.e., first portion) only of the fragility curve.

RESULTS

The total number of analyses carried out with reference to the entire bridge stock is considerable. 485 bridges times 90 simulations per bridge (9 intensity levels, i.e. average return periods, and 10 artificial motion samples per level) times two modeling assumptions (on the bearings) correspond to 81,000 IRHAs.

Figure 11 shows the final results with the computed median, 16% and 84% fractile fragility curves for damage and collapse on the left and right, respectively. The curves have been obtained by taking at each PGA level the corresponding fractiles of the exceedance probability.

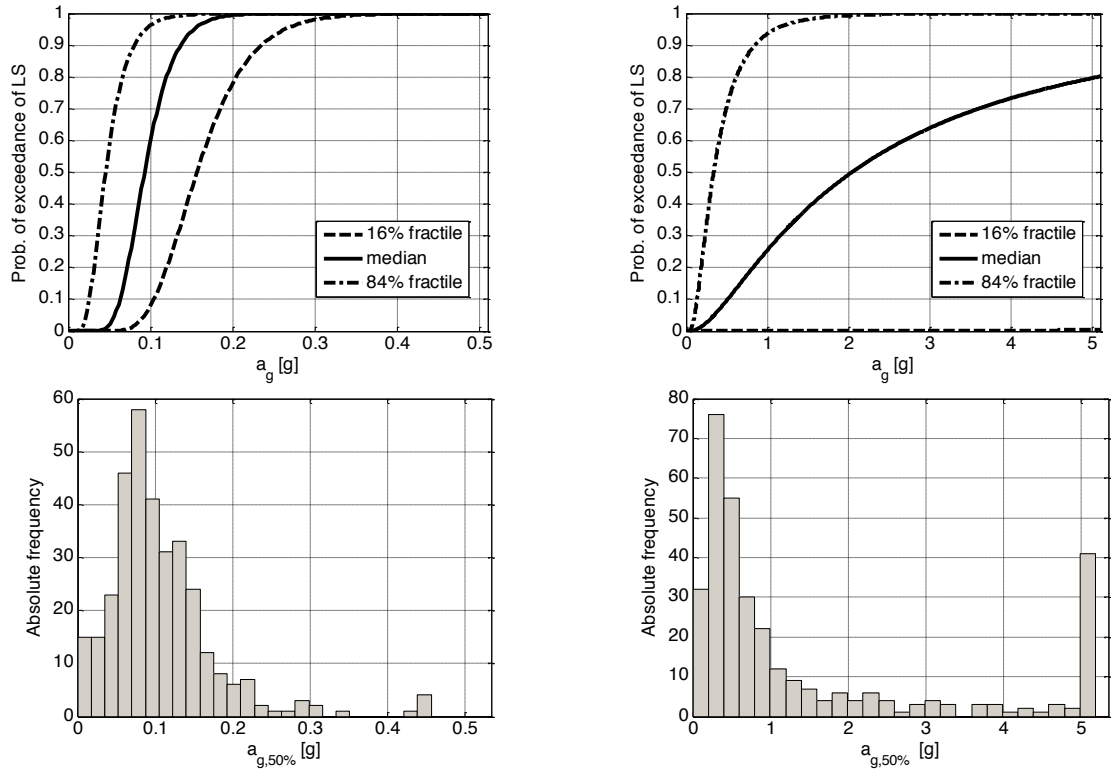

Figure 11. Computed median, 16% and 84% fractile fragility curves (first row) and histograms of absolute frequencies of the median PGA (50%) (second row) inducing damage (on the left) and collapse (on the right).

The figure reports also the histograms of relative frequencies of the median PGA (50%) inducing damage and collapse. A discussion on the differences to be found even within a reasonably uniform subset is given later with reference to Table 2. When the entire bridge stock is considered, as in Figure 11, the variability of capacity is impressive. In particular, for the collapse LS, the lowest fractile (16%) is almost flat. This is due to the fact that a considerable number of the bridges (41) has practically negligible collapse fragility with median collapse PGA well exceeding 5g (shown by a lump probability mass at 5g in the corresponding histogram): the results refer to the friction modeling assumption of older neoprene pad bearings, which fail, thus preserving the piers but not causing loss of support due to generally large support lengths. Mean curves have also been computed. For the purpose of connectivity analysis (scenario maps), the mean curves have been assigned to all girder bridges in the DB lacking data necessary for fragility analysis.

SEISMIC RISK MAPS

The risk λ_{LS}, i.e. the mean annual frequency (MAF) of exceeding a given structural limit state, is given by the usual integral:

$$\lambda_{LS} = \int_{-\infty}^{+\infty} p(LS|PGA = x)|d\lambda_{PGA}(x)| \tag{4}$$

where *p(LS|PGA)* is the fragility function for the LS and λ_{PGA} is the hazard curve (mean annual frequency of exceedance for PGA). Use of the lognormal distribution in Eq. (4) and for the whole fragility is common, well established choice but alternative shapes could be used. Also, statistical uncertainty in the parameter estimation ($\mu_{\ln Yj}$ and $\sigma_{\ln Yj}$) based on a finite, small number of IRHAs is not accounted for in the probability of Eq. (4).

To evaluate risk at the national level the probabilistic seismic hazard analysis study carried out in the INGV-DPC S1 project (esse1.mi.ingv.it), adopted by the Italian seismic design code was used. This study provides the already mentioned 16th, 50th and 84th fractiles of spectral acceleration values for a 0.05° × 0.05° grid of points and for 9 mean return periods. These data have been used to derive discrete-valued fractile hazard curves for PGA.

The MAF in Eq. (4) has been used to evaluate the unconditional damage and collapse probability for time windows t_d equal to 1, 10 and 50 years, respectively. Figure 12 shows two maps with collapse LS fragility values for a PGA characterized by T_R= 475 years (left) and the unconditional probability (risk) of exceeding the collapse LS in a time window of 50 years (right).

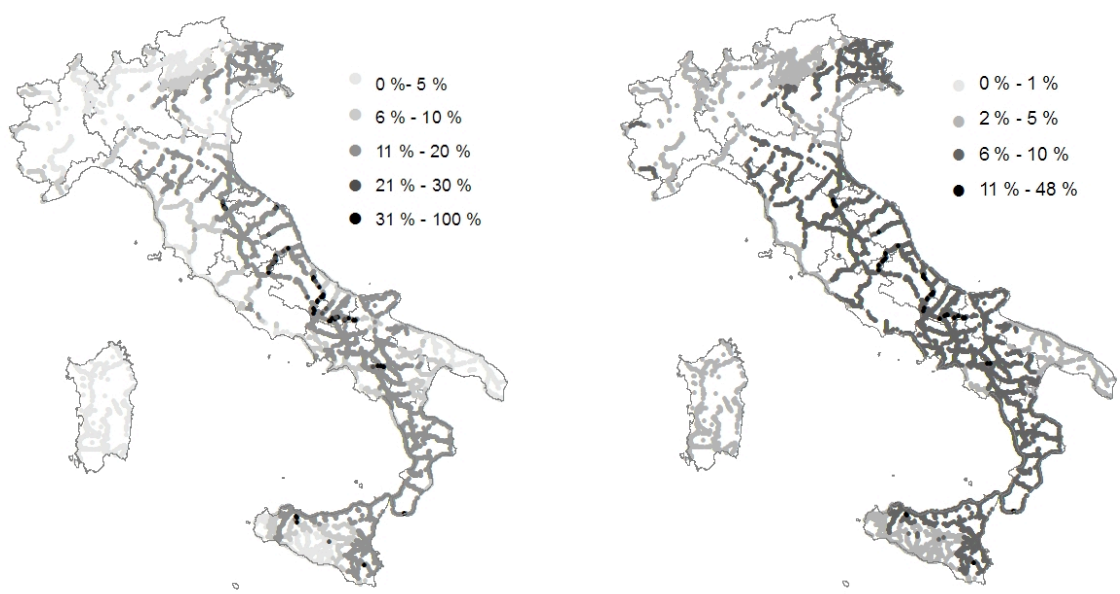

Figure 12. Maps showing the collapse LS fragility values for a PGA with T_R = 475 years (left) and the unconditional probability (risk) of exceeding the collapse LS in a time window of 50 years (right), for the median hazard curve.

REAL-TIME DAMAGE SCENARIO

In order to compute a real-time damage scenario the fragility curves are combined with shaking maps either coming from attenuation relationships or from records. Each bridge is then characterized by its fragility value at the predicted or measured (interpolated) PGA level. For the definition of shaking maps, four attenuation relationships have been selected from those recently published in the technical literature: Cauzzi and Faccioli (2008), Boore and Atkinson (2008), Akkar and Bommer (2010) and Bindi et al. (2011). With the exception of the Cauzzi and Faccioli (2008) attenuation law, the others account for the fault characteristics which can be selected from DISS DB (diss.rm.ingv.it/diss) of seismogenic sources affecting Italy, or directly input by the user. Once the magnitude, the epicenter and the focal depth are known, the ground shaking scenario at the site of each bridge up to a given distance from the epicenter can be evaluated. All four implemented attenuation laws are characterized by a simple form, which allows the generation of a damage scenario with a small amount of input data, and by a good performance witnessed by the match of predicted spectra with those derived from records of several Italian earthquakes (itaca.mi.ingv/ItacaNet).

Evaluation of real-time damage scenarios is one of the features implemented in the developed webGIS platform (described in the electronic supplement materials) and this tool has already been applied during two Civil Protection simulations carried out at regional level. In both cases, the real time damage scenario for bridges located within 50 km from the epicenter was computed. In addition, the network analysis tool integrated within the webGIS platform which exploits the Network Service of ESRI (esri.com) allows identifying the safest route for rescue teams to reach the hit areas (see Figure B-5 and Figure B-6 of the electronic supplement materials). The tool calculates the probability of reaching or exceeding a damage limit condition for the scenario earthquake. The user can then decide to identify a path that does not pass over bridges with a fragility higher than a selected acceptable failure probability.

FEASIBILIY EVALUATION OF A TYPOLOGICAL APPROACH FOR FRAGILITY DERIVATION

The damage and collapse fragility evaluated for 485 bridges within this project represents the largest set of consistently derived fragility curves available to date for bridge structures. Beside their direct use for risk analysis, they allow to obtain a clear indication on the

controversial issue of typological classification and the use of representative fragility functions.

For the sake of the discussion it is useful to recall the aggregation criteria employed in a number of works in order to define typologies and evaluate fragilities for a reduced set of bridges.

HAZUS (NIBS 1999) classifies bridges according to: seismic design (through spectrum modification factor, strength reduction factor due to cyclic motion, drift limits, and the longitudinal reinforcement ratio), number of spans (single vs. multiple span bridges), structure type (concrete, steel, others), pier type (multiple column bents, single column bents and pier walls), abutment type, bearing type (monolithic vs. non-monolithic; high rocker bearings, low steel bearings and neoprene rubber bearings), span continuity (continuous, discontinuous, i.e. with in-span hinges, simply supported). These criteria result in a total of 28 classes.

For Turkey, Avşar et al. (2011) identified span number (single vs multiple), bent column number (single vs multiple), and skew angle (negligible vs significant, chosen to be >30°) as the primary structural attributes for the analyzed ordinary bridges. As a result, the bridges, already quite uniform being all multiple-span RC structures with prestressed concrete girders and continuous cast-in-place decks, were subdivided into four classes (combination of bent column number and skew angle; single-span bridges were considered to be less vulnerable and were not included in the study).

Greek bridges, analyzed by Moschonas et al. (2009), were classified according to: deck type (slab, box-girder, simply supported prefabricated-prestressed girders with continuous RC slab), pier type (single-column cylindrical, rectangular, multiple column, wall-type) and deck-to-pier connection (monolithic, bearings and combination). Only 11 of the possible 36 typologies were considered (those with 5 or more bridges).

The database of bridges set up for the present study was queried with criteria that, according to all the classification schemes above, would correspond to a single typology to which a single set of fragility curves would be associated: multiple simply-supported spans, with single-stem hollow-core piers of height between 5m and 30m, and rubber bearings. The query retrieved 9 bridges, which are reported in Table 2.

Table 2 Properties of the bridges selected to have: multiple simply-supported spans, with single-stem hollow-core piers of height between 5m and 30m, and rubber bearings. Parameters of the fragility curves computed for this class of bridges.

						Damage		Collapse	
ID	year	# spans	L (m)	H_{min} (m)	H_{max} (m)	$PGA_{50\%}$ (g)	σ_{lnPGA}	$PGA_{50\%}$ (g)	σ_{lnPGA}
15	1980	7	236	6.60	14.6	0.10	0.28	0.67	0.44
127	1968	4	120	9.70	11.5	0.10	0.25	1.53	1.47
128	1968	4	120	9.70	11.3	0.10	0.24	1.75	1.43
296	‘70s	6	207	5.95	12.6	0.20	0.31	0.79	0.69
310	1973	12	425	6.10	17.1	0.13	0.30	0.36	0.52
321	‘80s	6	211	9.80	13.0	0.18	0.08	0.70	0.75
343	‘70s	8	269	7.00	20.0	0.15	0.35	2.41	1.62
376	‘70s	9	305	9.90	26.1	0.11	0.20	1.02	0.94
377	‘70s	13	448	8.00	28.9	0.11	0.19	0.18	0.77

Table 2 shows also that the bridges are uniform in terms of design code, since they date from 1968 to the ‘80s (a period over which the seismic code remained substantially unchanged). Damage and collapse fragility curves are shown in Figure 13 (parameters in the table). As it can be easily seen from the figure and quantitatively appreciated from the table, the median value within this small set of supposedly uniform bridges varies of 100%, from a minimum of 0.10g to a maximum of 0.20g (with a c.o.v. of the median of 28%) for the damage LS, and of more than 1200%, from a minimum of 0.18g to a maximum of 2.41g (with a c.o.v. of 69%) for the collapse LS.

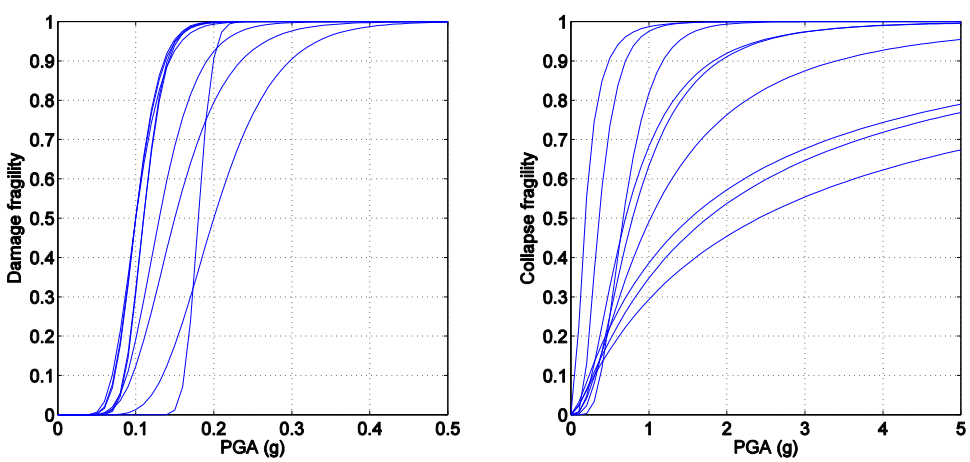

Figure 13. Derived fragility curves for the selected 9 bridges: damage (left) and collapse (right).

In spite of its limited scope this exploration is deemed to be already sufficient to put into question the feasibility of a typological approach for fragility derivation. While its use can be probably still justified for buildings, where fragility curves are usually employed in portfolio

loss assessment studies, every bridge plays a specific function at a specific location within a networked system, which requires a much greater accuracy of evaluation.

CONCLUSIONS

The final goal of the presented research is the evaluation of seismic risk of the bridge stock on the Italian roadway network. The paper illustrates the tools developed, with a focus on the largest typology in the stock, i.e. RC girder bridges. Data of about 17,000 bridges were collected from different nonhomogeneous sources (private and public owners, concessionaires, etc.) and introduced in a unified relational DB. The quality of the available information is not uniform and a complete data set (structural) was available for 485 bridges. A software tool (BRI.T.N.E.Y.) was developed in order to treat information relative to an unusually large stock of bridges in a fully automatic, consistent and accurate way for numerically evaluating their seismic fragilities. Bridge-specific fragility curves were computed for the sub-set of 485 bridges for two limit states: damage and collapse. The results obtained for these bridges were then statistically extended to bridges with an incomplete set of data in order to allow a provisional estimate of: a) seismic risk at a national scale for the purpose of retrofit prioritization and b) the evaluation of real-time damage and accessibility scenarios. A webGIS platform was developed for storing and visualizing available data and results in terms of seismic risk maps, performing real-time damage scenarios and network analyses. The platform was tested by Italian Civil Protection during two regional simulations and it's ready to be used in real-life applications.

Further developments are possible and of straightforward implementation within the current application framework. The most important ones refer to the seismic input model, which is regarded as the only aspect where an expert human operator would make a real difference with respect to the developed application. In order of importance, these are the use of natural recorded motions, the modeling of non uniform input (with conditional sampling from the natural motions) and the inclusion of SSI. The strength of the application is that once the above extensions will be implemented, or robust degrading hysteretic models will be available, or new data will be collected, it will be possible to automatically re-analyze the entire bridge stock of the country and update the fragility curves.

Additional enrichment of this study will be related to the integration of these results with the seismic risk of other fundamental structures of the road transportation system such as

tunnels and retaining walls, and with the indirect geotechnical risk associated with earthquake-triggered landslides.

ACKNOWLEDGMENTS

This work was supported by the Italian Civil Protection Department within the framework of the "Seismic risk of the national road transportation network" Project (Progetto Operativo d4). This support is gratefully acknowledged. Any opinions, findings or conclusions expressed in this paper are those of the authors and do not necessarily reflect those of the Department. The authors thank M. Onida, A. Di Meo, T. Scappaticci, R. Iaccino and the staff of the "Vulnerability and territorial management" research area of EUCENTRE for the valuable input to the work described in this paper.

REFERENCES

Akkar, S., Bommer, J.J., 2010. Empirical equations for the prediction of PGA, PGV, and spectral accelerations in Europe, the Mediterranean Region, and the Middle East, *Seismological Research Letters* **81(2)**, 195-206.

Avşar, Ö, Yakut, A., and Caner, A. 2011. Analytical Fragility Curves for Ordinary Highway Bridges in Turkey, *Earthquake Spectra* **27(4)**, 971–996.

Baradaran Shoraka, M., Yang, T. Y., Elwood, K. J., 2013. Seismic loss estimation of non-ductile reinforced concrete buildings, *Earthquake Engineering and Structural Dynamics* **42**, 297–310.

Bindi, D., Pacor, F., Luzi, L., Puglia, R., Massa, M., Ameri, G., Paolucci, R., 2011. Ground motion prediction equations derived from the Italian strong motion database, *Bulletin of Earthquake Engineering* **9(6)**, 1899-192.

Biskinis, D. E., and Fardis, M. N., 2010a. Flexure-controlled ultimate deformations of members with con- tinuous or lap-spliced bars, *Structural Concrete* **11(2)**, 93–108.

Biskinis, D. E., and Fardis, M. N., 2010b. Deformations at flexural yielding of members with continuous or lap-spliced bars, *Structural Concrete* **11(3)**, 127-138.

Biskinis, D., Roupakias, G., and Fardis, M.N., 2004. Degradation of Shear Strength of RC Members with Inelastic Cyclic Displacements, *ACI Structural Journal* **101(6)**, 773-783.

Bommer, J.J., and Acevedo, A.B., 2004. The use of real earthquake accelerograms as input to dynamic analysis, *Journal of Earthquake Engineering* **8(S1)**, 43-91.

Booch, G., Maksimchuk, R. A., Engle, M. W., Young, B. J., Conallen, J., and Houston, K.A., 2007. *Object-Oriented Analysis and Design with Applications*. Third Edition. Addison Wesley.

Boore, D.M., and Atkinson, G.M., 2008. Ground motion prediction equations for the average horizontal component of PGA, PGV, and 5%-damped PSA at spectral periods between 0.01 and 10.0 s, *Earthquake Spectra* **24**, 99-138.

Bradley, B., 2013, *Ground motion selection for seismic risk analysis of civil infrastructure*, Handbook of seismic risk analysis and management of civil infrastructure systems (Tesfamariam and Goda eds), Woodhead Publ. Ltd, UK, ISBN 978-0-85709-268-7.

Calvi, G. M., Pinto, P. E., Franchin, P., and Marnetto, R. 2010. The highway network in the area struck by the event" *Progettazione Sismica* **1(3)**, Special Issue on the April 6th 2009 l'Aquila earthquake IUSSPress, Pavia, Italy.

Calvi, G. M., Pinto, P. E., and Franchin, P., 2013. *Seismic design practice in Italy*, in Bridge Engineering Handbook 2nd edition: Seismic design, Editors: Chen W-F and Duan L, CRC-Press, ISBN 9781439852187.

Capozzi, V., 2009. Seismic behavior of connections in prefabricated structures. *PhD Thesis*, Department of Structural Engineering, University of Naples "Federico II" (in Italian).

Cauzzi, C., and Faccioli, E., 2008. Broadband (0.05 to 20 s) prediction of displacement response spectra based on worldwide digital records, *Journal of Seismology* **12(4)**, 453-475.

DM 14/01/2008, 2008. New Technical Norms for Constructions. Official Gazetteer of the Italian Republic 04.02.2008 n.29.

Dolsek, M., 2009. Incremental dynamic analysis with consideration of modeling uncertainties, *Earthquake Engineering & Structural Dynamics* **38**, 805–825.

EC8, 2005. *Eurocode 8. Design of structures for earthquake resistance – Part 3: Strengthening and repair of buildings*.

Elwood, K., 2004. Modeling failures in existing reinforced concrete columns, *Canadian Journal of Civil Engineering* **31**, 846-859.

Franchin, P., and Pinto, P.E., 2009. Allowing traffic over mainshock-damaged bridges, *Journal of Earthquake Engineering* **13**, 585-599.

Franchin, P., Pinto, P. E., and Calvi, G. M., 2013. Bridges and road network, *Progettazione Sismica* **5**, Special Issue on the May 22nd 2012 Emilia earthquake, IUSSPress, Pavia, Italy.

Fenves, G. L., 1990. Object-Oriented Programming for Engineering Software Development, *Engineering with Computers* **6**, 1-15.

Gamma, E., Helm, R., Johnson, R., Vlissides, J., 2003. Elements of Reusable Object-Oriented Software, Design Patterns CD, Foreword by Grady Booch. Addison Wesley Longman, Inc.

Gardoni, P., Der Kiureghian, A., and Mosalam, K. M., 2002. Probabilistic capacity models and fragility estimates for reinforced concrete columns based on experimental observations, *Journal of Engineering Mechanics* **128(10)**, 1024–1038.

Gazetas, G., Fan, K., and Kaynia, A., 1993. Dynamic response of pile groups with different configurations, *Soil Dynamics and Earthquake Engineering* **12**, 239–257.

GNDT, 2000. VIA Project – Reduction of the seismic vulnerability of infrastructural networks and environment,ftp.ingv.it/pro/gndt/Att_scient/Prodotti_consegnati/prodotti_elenco_progetti_con_int .htm (in Italian).

Haselton, C. B., Liel, A., Deierlein, G. G., Dean, B. S., and Chou, J. H., 2011. Seismic Collapse Safety of Reinforced Concrete Buildings. I: Assessment of Ductile Moment Frames. *ASCE Journal of Structural Engineering* **137**, 481-491.

Haselton, C. B., Liel, A. B., Taylor Lange, S., and Deierlein, G. G., 2008. *Beam-column element model calibrated for predicting flexural response leading to global collapse of RC frame buildings*, Pacific Earthquake Engineering Centre, PEER 2007/03.

Iervolino, I., Galasso, C., and Cosenza, E., 2010. REXEL: computer aided record selection for code-based seismic structural analysis, *Bulletin of Earthquake Engineering* **8**, 339–362.

Jalayer, F., and Cornell, C. A., 2009. Alternative nonlinear demand estimation methods for probability-based seismic assessments, *Earthquake Engineering & Structural Dynamics* **38**: 951-972.

Jalayer, F., Franchin, P., and Pinto, P.E., 2007. A scalar damage measure for seismic reliability analysis of RC frames, *Earthquake Engineering & Structural Dynamics* **36(13)**, 2059-2079.

Kowalsky, M. J., and Priestley, M. J. N., 2000. Improved Analytical Model for Shear Strength of Circular Reinforced Concrete Columns in Seismic Regions, *ACI Structural Journal* **97(3)**, 388-396.

Liel, A. B., Haselton, C. B., Deierlein, G. G., and Baker, J. W., 2009. Incorporating modeling uncertainties in the assessment of seismic collapse risk of buildings, *Structural Safety* **31**, 197-211.

Lin, T., Haselton, C. B. and Baker, J. W., 2013. Conditional spectrum-based ground motion selection. Part I: Hazard consistency for risk-based assessments, *Earthquake Engineering & Structural Dynamics* **42(12)**, 1847-1865.

Mackie, K.R., and Stojadinovic, B., 2007. R-factor parameterized bridge damage fragility curves, *Journal of Bridge Engineering* **12**, 500-510.

Mander, J. B., and Basöz, N., 1999. Seismic fragility curve theory for highway bridges in transportation lifeline loss estimation, in Optimising post-earthquake lifeline system reliability, *TCLEE Monograph 16*, eds Elliot and McDonough, 31-40.

McKenna, F., Scott, M. H., and Fenves, G. L., 2010. Nonlinear Finite-Element Analysis Software Architecture Using Object Composition, *Journal of Computing in Civil Engineering* **24(1)**, 97-105.

MIDAS Civil, 2011. MIDAS Information Technology Co., Ltd http://www.cspfea.net/midas_civil.php.

Moschonas, I. F., Kappos, A. J., Panetsos, P., Papadopoulos, V., Makarios, T., and Thanopoulos, P., 2009. Seismic fragility curves for Greek bridges: methodology and case studies, *Bulletin of Earthquake Engineering* **7**, 439-468.

Muscolino, G., 2002. *Dynamics of Structures*, Milan, McGraw-Hill (in Italian).

Nebbia, G., and Pardi, L., 2008. The SAGGI project: advanced systems for global management of an infrastructure *Autostrade Editore* 2/2008 (in Italian).

NIBS (National Institute of Building Sciences), 1999. Earthquake loss estimation methodology: HAZUS99 (SR2), Technical manual, Federal Emergency Management Agency, Washington, DC URL: http://www.fema.gov/hazus.

Pinto, P. E., and Franchin, P., 2010. Issues in the upgrade of Italian highway structures. *Journal of Earthquake Engineering* **14**, 1221-1252.

Pinto, P.E., Giannini, R., and Nuti, C., 1996. Seismic risk evaluation of the highway network in its present states, identification of intervention priorities and of the upgrade measures for bridges. *Autostrade Editore,* Repertorio n. 16203 (in Italian).

Pinto, P.E., and Mancini, G., 2009. Seismic assessment and retrofit of existing bridges. *Proceedings of the Final Workshop of the 2005-2008 ReLuis-DPC Project* (in Italian), Naples, Italy.

Scott, M. H., and Fenves, G. L., 2006. Plastic Hinge Integration Methods for Force-Based Beam-Column Elements, *Journal of Structural Engineering ASCE* **132(2)**, 244–252.

Sextos, A. G., Pitilakis, K. D. and Kappos, A. J., 2003a. Inelastic dynamic analysis of RC bridges accounting for spatial variability of ground motion, site effects and soil–structure interaction phenomena. Part 1: Methodology and analytical tools. *Earthquake Engineering & Structural Dynamics* **32**, 607–627.

Sextos, A. G., Pitilakis, K. D., and Kappos, A. J., 2003b. Inelastic dynamic analysis of RC bridges accounting for spatial variability of ground motion, site effects and soil–structure interaction phenomena. Part 2: Parametric study. *Earthquake Engineering & Structural Dynamics* **32**, 629–652.

Taherzadeh, R., Clouteau, D., and Cottereau, R., 2009. Simple formulas for the dynamic stiffness of pile groups. *Earthquake Engineering & Structural Dynamics* **38**, 1665–1685.

Vamvatsikos, D., and Cornell, C. A., 2002. Incremental Dynamic Analysis, *Earthquake Engineering & Structural Dynamics* **31**, 491–514.

Wolf, J.P., 1991. Consistent lumped-parameter models for unbonded soil: physical representation. *Earthquake Engineering & Structural Dynamics* **20**, 12–32.

Zhu, L., Elwood, K. J., and Haukaas, T., 2007. Classification and seismic safety evaluation of existing reinforced concrete columns, *Journal of Structural Engineering* **133(9)**, 1316–1330.